APRIL 01 2003

Mechanisms of lesion formation in high intensity focused ultrasound therapy

Wen-Shiang Chen; Cyril Lafon; Thomas J. Matula; Shahram Vaezy; Lawrence A. Crum

ARLO 4, 41–46 (2003)
https://doi.org/10.1121/1.1559911

Mechanisms of lesion formation in high intensity focused ultrasound therapy

Wen-Shiang Chen, Cyril Lafon, Thomas J. Matula, Shahram Vaezy, and Lawrence A. Crum

Center for Industrial and Medical Ultrasound, Applied Physics Lab., University of Washington, Seattle, WA 98105
wschen@u.washington.edu, lafon@lyon151.inserm.fr, matula@apl.washington.edu, vaezy@apl.washington.edu, lac@apl.washington.edu

Abstract: The lesions generated by high intensity ultrasound were studied in transparent tissue phantoms premixed with and without ultrasound contrast agents (UCA) at 1.1- and 3.5-MHz acoustic waves. Generation of small bubbles was observed at the very beginning of exposure, whereas cigar-shaped thermal lesions began to form at the focus after a delay. After further heating, boiling occurred and changed the lesion to tadpole-shape, with advancement toward the transducer. Broadband noise was detected in phantoms with UCA initially. UCA also lowered the pressure threshold and enlarged the lesion. Although thermal and cavitation effects are believed to be both important in lesion formation, tadpole-shaped transformation results from boiling activity.

PACS number: 43.80.Gx, 43.80.Sh
Date received: 17 February 2002 **Date accepted**: 8 December 2002

1. Introduction

The minimally invasive nature of high intensity focused ultrasound (HIFU) has been a focus of different therapeutic applications recently, especially tumor ablation [Sanghvi *et al.*, 1999, He *et al.*, 2001, Chapelon *et al.*, 1999, Daum *et al.*, 1999, ter Haar, 2001, Vaezy *et al.*, 2001, Wu *et al.*, 2001]. However, in some cases the lesions were not formed as expected, either in shape, or in location relative to the geometric focus [Watkin *et al.*, 1996, Bailey *et al.*, 2001]. Theoretically, for a pure thermal process, the lesion should be cigar-shaped and centered around the transducer focus. This shape corresponds to the focal area (full-width, half intensity) and thus the area of highest thermal deposition. The unexpected experimental observations cannot be explained sufficiently either by nonlinear wave propagation or by the changes in the acoustic properties of the denaturing tissue. The presence of bubbles was proposed to be the main reason [Meaney *et al.*, 2000, Chavrier *et al.*, 2000, Bailey *et al.*, 2001]. However, whether these bubbles are generated by inertial cavitation or boiling is still unknown.

Recently, a transparent tissue-mimicking phantom was developed in our laboratory, which provides two unique benefits: (1) real-time visualization of HIFU-induced lesions; and (2) adjustable attenuation by varying the protein concentration [Lafon *et al.*, 2002]. This special phantom gives us a chance to understand the mechanism of HIFU lesion formation. Our goals in this study are: (1) to observe in real time the HIFU lesion formation process at different intensity levels; (2) to study the mechanism of the 'tadpole-shaped' lesion transformation; (3) to evaluate the role of inertial cavitation (IC) and tissue boiling in the lesion formation process; (4) and to investigate the change of lesion size, pressure threshold, and mechanism of lesion formation after the addition of ultrasound contrast agent (UCA).

2. Method

Our phantom is based on polyacrylamide gel mixed with Bovine Serum Albumin (BSA), a protein used as a temperature-sensitive indicator. HIFU-induced denaturation was easily observable and highly contrasted. The attenuation of this material can be adjusted with the BSA concentration. We used a 7% BSA, which gives a gel with an acoustic attenuation of 0.017 Np/cm/MHz. The sound speed and material density, which are independent of the protein concentration, are 1544 m/s and 1044 kg/m^3 respectively [Lafon *et al.*, 2001]. The mixture was poured into a 30-ml plastic cell, sealed with a parafilm membrane, and gently agitated for 30 min. Afterwards, the cell (with the parafilm membrane removed) was mounted on a positioning system (Velmex, Bloomfield, NY) and immersed in a water-filled tank.

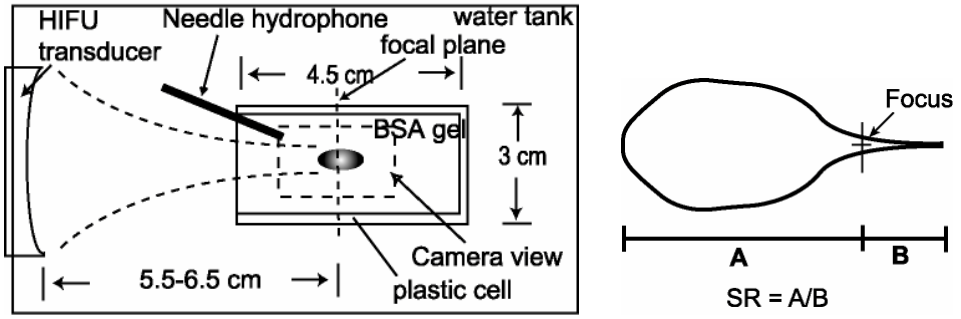

Fig. 1. (a) Experiment setup; (b) definition of symmetric ratio (SR).

Ultrasound energy was delivered through the opened top of the cell either by a 1.1 MHz (f = 1.0) or a 3.5 MHz (f = 1.6) transducer (Sonic Concepts, Woodinville, WA) operating in continuous wave (CW) mode. The total exposure time was 90 seconds. We used longer exposure times compared with other HIFU studies [Watkin *et al.*, 1996, Clarke *et al.*, 1997, Chavrier *et al.*, 2000, Holt *et al.*, 2001], since we want to see the lesion formation at different pressure levels, from just above the lesion formation threshold to a high level. In low pressure situations, the lesion formation took a longer time, and transformation might not occur at all. The focus of the HIFU transducer was set at the center of the sample cell. A Polyvinylidene fluoride (PVDF) needle hydrophone was inserted into the cell through the top side to monitor the scattered signal (Fig. 1a). Gel phantoms with and without Sonazoid^{TM} UCA (mean diameter 2.17μm) were exposed to a preselected pressure level ranging from 3 to 5.2 MPa (intensity: 1400 to 2000 W/cm^2). The concentration of the UCA was about 10 bubbles/mm^3. Real-time lesion formation process was recorded by a charge-coupled-device (CCD) camera and video cassette recorder (VCR). The recorded images were digitized and processed by a procedure written in Matlab (Math Works, Natick, MA). To quantify the shape transformation of lesions, we measured the symmetric ratio (SR), which was defined as the length of the lesion in front of the focus divided by the length behind (Fig. 1b).

3. Results

Movie clip 1 and 2 (Mm. 1, 2) show the real-time formation of HIFU lesions at the two different frequencies, 1.1 (Fig. 2a) and 3.5 MHz (Fig. 2b). The HIFU transducer (not shown) is located on the left side of these images. The beginning of the HIFU exposure is indicated by a green LED (in movies only). The elapsed time is displayed on the upper left corner.

Mm. 1. Lesion formed at 1.1MHz (1.4 MB) [292.01.mpg]

Mm. 2. Lesion formed at 3.5MHz (1.4 MB) [292.02.mpg]

In this first set of experiments, no UCA was mixed in the phantom. In Fig. 3 (or Mm. 1, 0 sec.), small white reflective dots were observed immediately after switching on the HIFU

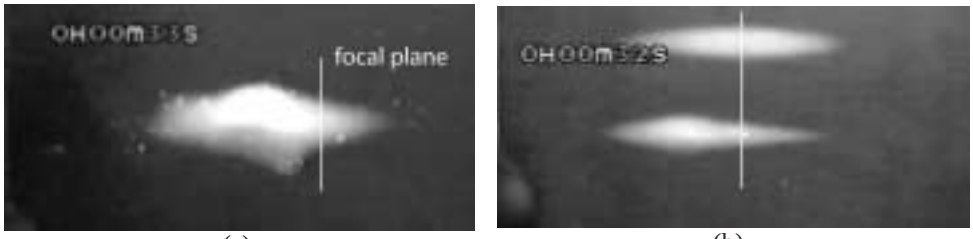

Fig. 2. (a) Tadpole-shaped lesion formation and boiling at 1.1 MHz (P.=5.4MPa); (b) upper: cigar-shaped lesion at P.=3.2MPa; lower: tadpole-shaped lesion formed at P.=3.8 MPa. (1.1MHz).

Fig. 3. Bubbles (white dots) created by IC at the beginning of the HIFU exposure (1.1 MHz, 0 sec.).

transducer operating at 1.1 MHz. No reflective dots were seen at the beginning of 3.5 MHz (Mm. 2) exposure. At a frequency of 1.1 MHz, the thermal lesion developed after 12s of exposure (cigar-shaped). Boiling-like activity was initially observed after 20s of exposure, and more vigorous activity (Fig. 2a) was seen after 30s. Passive cavitation detection (PCD) measurements during the vigorous activity revealed no broadband noise, and suggested that boiling, instead of IC from preexisting microbubbles, occurred. The delay onset of the boiling-like activity further suggested that thermal effects, rather than preexisting microbubble cavitation, is responsible for the vigorous bubble creation. The lesions changed from cigar to tadpole shape after boiling. At 3.5 MHz, the lesions remained cigar shaped for low pressure levels (3.2 MPa) (Fig. 2b, upper lesion). However, when the pressure was increased to 3.8 MPa, the lesion transformed to a tadpole shape at 11s soon after vigorous

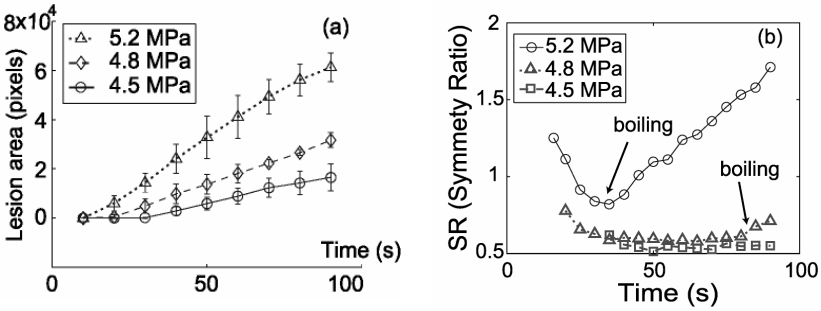

Fig. 4. (a) Pressure vs. lesion size at 1.1MHz. The final lesion was larger at higher pressures; (b) change of SR for three selected lesions at different pressure levels for the three pressures in (a). Note here that at 4.5 MPa, there was no boiling observed. The lesion was cigar-shaped. The SR 'rose' after the boiling effect.

boiling. A sequence of explosion-like events most likely related to boiling forced the lesion to move rapidly toward the transducer.

Figure 4a shows the effect of pressure on the lesion formation process for a frequency of 1.1 MHz. Results of measurements at three pressure levels, 4.5, 4.8, and 5.2 MPa are shown. Boiling phenomenon was seen both at 4.8 and 5.2, but not at 4.5 MPa. A longer exposure time is probably needed to induce boiling at 4.5 MPa. The lesion size increased gradually, and the rate was not altered when boiling occurred. Higher pressure levels generated larger lesions. However, for the same pressure levels, the symmetry ratio (SR) of the formed lesion increased when boiling occurred (Fig. 4b, 4.8 and 5.2 MPa). The cigar-shaped lesion formed at 4.5 MPa had a SR stabilized at around 0.55. At 5.2 and 4.8 MPa, boiling and SR increase occurred after 38s and 82s of exposure respectively.

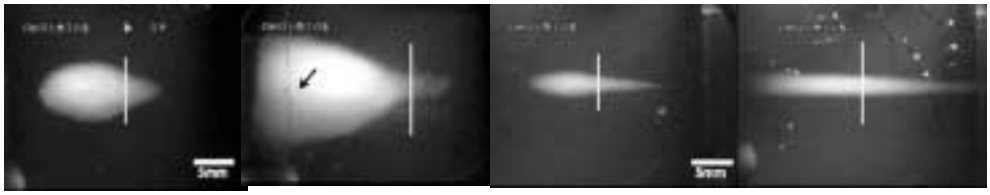

(a) (b) (c) (d)

Fig. 5. Lesions formed for phantoms without UCA (a, c), with UCA (b, d), at 1.1 (a, b) and 3.5 MHz (c, d) at P.= 4.8 MPa. Black arrow in (b) indicates the initial point of lesion formation.

After adding UCA, the pressure threshold for lesion formation was about 1MPa lower at 1.1MHz. No significant change in this threshold was observed at 3.5 MHz. For this case, unlike the phantom without UCA, the lesion was formed by merging numerous small white dots and started at a position in front of the focus (Fig. 5b, arrow). That is, the lesion started from the head part of the final lesion shown in Fig. 5b, grew larger, and extended backward toward the focus (white line). Although the lesions formed in gel with UCA at 90 seconds looked tadpole-shaped, they didn't experience the symmetric growth, boiling, shape transformation, and migration process. It is probably reflecting the beam shape of the transducer itself. Boiling was not seen at either frequencies, but the lesion size increased significantly (Figs. 5b and 5d). At 3.5MHhz, the lesion started as a long lesion and quickly extended toward and away from the transducer simultaneously (Fig. 5d).

Figure 6 shows the frequency spectrum of the signal recorded by needle hydrophone, which verified that boiling, but not preexisting bubble cavitation, was responsible for tadpole lesions. Except for the fundamental frequency (1.1 MHz) and harmonics, typical broadband noise from approximately 2 to 6 MHz was seen for the phantom with UCA (Fig. 6b), but not for the phantom without UCA (Fig. 6a). During the vigorous boiling process in phantoms without UCA, no broadband noise pattern was observed. In phantoms with UCA, the broadband noise occurred in the first few seconds and died out fast (Fig. 6c), whereas the lesion enlarged in the whole exposure. Intermittent bursts of activity were seen occasionally. At 3.5MHz, no broadband noise was recorded during the entire exposure period in both samples with and without UCA.

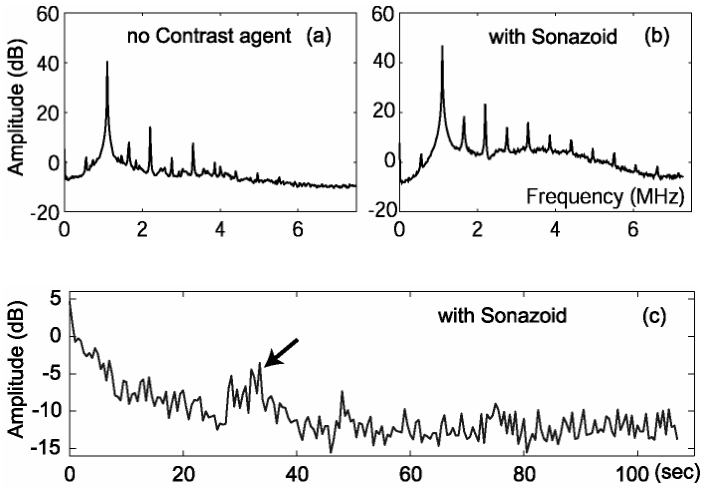

Fig. 6. Frequency spectrums of the recorded signal at 1.1MHz. (a) First 2s in phantom without UCA; (b) in phantom with UCA; (c) peak amplitude of the broadband noise. Arrow: intermittent burst of broadband noise.

4. Discussion

Two possible sources of bubbles could be used to explain the tadpole-shaped lesion formation and advancement during HIFU therapy. First, bubbles are in situ or generated by IC from existing nuclei [Holt *et al.*, 2001]. Chavrier's simulation estimated that at 2.25 MHz and intensity level of 4300 W/cm^2, tadpole-shaped lesions will be generated when the concentration of micrometer-sized bubbles is greater than 500 bubbles/mm^3 [Chavrier *et al.*, 2000]. In our phantoms with UCA at a concentration of 10 bubbles/mm^3, the existing UCA was apparently already enough to impede the sound transmission and force the lesion to start centimeters in front of the focus (at 1.1MHz). Therefore, one would expect that a high concentration of bubbles should be nucleated and concentrated at the focal area only. However, no broadband noise was detected in our phantoms without UCA at the onset of lesion formation or transformation. Note also that degassing agar gel failed to change the pressure threshold of enhanced heating [Holt *et al.*, 2001]. The second possibility assumes that the bubbles are created from tissue boiling at the focus. In our observations, pressure dependent IC did occur at the beginning of exposure and created bubbles. These bubbles undergoing IC could deposit enough heat [Holt *et al.*, 2001] to denature the surrounding albumin and turn it white. However, the subsequent lesion formation did not originate from these white dots. Cigar-shaped lesions started near the geometric focus. Also, boiling-like activity and lesion transformation occurred much later than the generation of white dots and is therefore considered to be a separate process (Fig. 4b). Similar white dots, but in greater number, were observed for the initial few seconds in phantoms with UCA at 1.1MHz, when broadband noise was detected. Lesions were formed by the apparent merging of these numerous white dots. At 3.5MHz, elongated tadpole-shaped lesions were formed after adding UCA. Not enough bubbles were generated by IC to effectively block the sound transmission.

The presence of bubbles might be beneficial to the HIFU therapy. Attempts have been made to use UCA to facilitate the lesion formation process. Tran *et al.* introduced UCA to the target tissue and showed the reduction of the threshold intensity for lesion formation and the requisite duration of HIFU therapy [Tran *et al.*, 2002]. Fry *et al.* reported the transportation of microbubbles formed during the HIFU therapy through vessels and suggested the potential of enhancing tissue debulking under controlled conditions. However, escaping vapor bubbles might also induce unwanted vessel rupture and lesion formation

outside the target area by either inertial collapse or enhanced heating of bubbles [Fry *et al.*, 1995]. The shift of maximal heating region, such as the case of our UCA-mixed phantoms, might also compromise important nearby structure in front of the focus.

Lesion formation during HIFU therapy is a complicated process, which involves both thermal and cavitation effects. The initial lesion is formed thermally. Boiling of the tissue causes the lesion shape transformation and advancement. In phantoms premixed with UCA, the enhanced heating from IC-generated bubbles is the dominant mechanism for lesion formation, especially at low frequency.

Acknowledgments

This work was supported in part by NSF #BES-0002932 and NIH #8R01 EB003500-02.

References and links

Bailey, M. R., Couret, L. N., Sapozhnikov, O. A., Khokhlova, V. A., ter Haar, G., Vaezy, S., Shi, X., Martin, R., and Crum, L. A. **(2001)**. "Use of overpressure to assess the role of bubbles in focused ultrasound lesion shape in vitro," Ultrasound Med. Biol. **27,** 695-708.

Chapelon, J. Y., Ribault, M., Vernier, F., Souchon, R., and Gelet, A. **(1999)**. "Treatment of localised prostate cancer with transrectal high intensity focused ultrasound," Eur. J. Ultrasound **9,** 31-38.

Chavrier, F., Chapelon, J. Y., Gelet, A., and Cathignol, D. **(2000)**. "Modeling of high-intensity focused ultrasound-induced lesions in the presence of cavitation bubbles," J. Acoust. Soc. Am. **108,** 432-440.

Clarke, R. L., and ter Haar, G. R. **(1997)**. "Temperature rise recorded during lesion formation by high-intensity focused ultrasound," Ultrasound Med. Biol. **23,** 299-306.

Daum, D. R., Smith, N. B., King, R., and Hynynen, K. **(1999)**. "In vivo demonstration of noninvasive thermal surgery of the liver and kidney using an ultrasonic phased array," Ultrasound Med. Biol. **25,** 1087-1098.

Fry, F. J., Sanghvi, N. T., Foster, R. S., Bihrle, R., and Hennige, C. **(1995)**. "Ultrasound and microbubbles: their generation, detection and potential utilization in tissue and organ therapy--experimental," Ultrasound Med. Biol. **21,** 1227-1237.

He, S. X., Xiong, L. L., Yao, S. S., Yu, J. S., Lan, J. M. X., He, C. J., Shan, S. S., Zeng, J. Q., Zang, Y., and Du, R. U. **(2001)**. "Early clinical study of high intensive focused ultrasound in the treatment of 160 patients with advanced abdominal and pelvic malignant tumors and hypertrophy," Chin. Med. J. (Engl) **114**, http://www.cmj.org/heshengxu2.htm.

Holt, R. G., and Roy, R. A. **(2001)**. "Measurements of bubble-enhanced heating from focused, MHz-frequency ultrasound in a tissue-mimicking material," Ultrasound Med. Biol. **27,** 1399-1412.

Lafon, C., Vaezy, S., Noble, M., Kaczkowski, P. J., Martin, R., and Crum, L. A. **(2002)**. "A new synthetic tissue-mimicking phantom for high intensity focused ultrasound," 2001 Proc. IEEE Ultrason. Symp. **2,** 1295-1298.

Meaney, P. M., Cahill, M. D., and ter Haar, G. R. **(2000)**. "The intensity dependence of lesion position shift during focused ultrasound surgery," Ultrasound Med. Biol. **26,** 441-450.

Sanghvi, N. T., Foster, R. S., Bihrle, R., Casey, R., Uchida, T., Phillips, M. H., Syrus, J., Zaitsev, A. V., Marich, K. W., and Fry, F. J. **(1999)**. "Noninvasive surgery of prostate tissue by high intensity focused ultrasound: An updated report," Eur. J. Ultrasound **9,** 19-29.

ter Haar, G. R. **(2001)**. "High intensity focused ultrasound for the treatment of tumors," Echocardiography. **18,** 317-322.

Tran, B. C., Seo, J., Fowlkes, J. B., and Cain, C. A. **(2002)**. "Microbubble enhanced threshold reductions for tissue damage using high intensity ultrasound," 2001 Proc. IEEE Ultrason. Symp. **2,** 1389-1392.

Vaezy, S., Shi, X., Martin, R. W., Chi, E., Nelson, P. I., Bailey, M. R., and Crum, L. A. **(2001)**. "Real-time visualization of high-intensity focused ultrasound treatment using ultrasound imaging," Ultrasound Med. Biol. **27,** 33-42.

Watkin, N. A., ter Haar, G. R., and Rivens, I. **(1996)**. "The intensity dependence of the site of maximal energy deposition in focused ultrasound surgery," Ultrasound Med. Biol. **22,** 483-491.

Wu, F., Chen, W. Z., Bai, J., Zou, J. Z., Wang, Z. L., Zhu, H., and Wang, Z. B. **(2001)**. "Pathological changes in human malignant carcinoma treated with high-intensity focused ultrasound," Ultrasound Med. Biol. **27,** 1099-1106.